

Simulating seeded vacuum decay in a cold atom system

Thomas P. Billam,^{1,*} Ruth Gregory,^{2,3,†} Florent Michel,^{2,‡} and Ian G. Moss^{4,§}

¹Joint Quantum Centre (JQC) Durham–Newcastle, School of Mathematics,

Statistics and Physics, Newcastle University, Newcastle upon Tyne, NE1 7RU, UK

²Centre for Particle Theory, Durham University, South Road, Durham, DH1 3LE, UK

³Perimeter Institute, 31 Caroline Street North, Waterloo, ON, N2L 2Y5, Canada

⁴School of Mathematics, Statistics and Physics, Newcastle University, Newcastle upon Tyne, NE1 7RU, UK

(Dated: April 2, 2019)

We propose to test the concept of seeded vacuum decay in cosmology using a Bose-Einstein condensate system. The role of the nucleation seed is played by a vortex within the condensate. We present two complementary theoretical analyses that demonstrate seeded decay is the dominant decay mechanism of the false vacuum. First, we adapt the standard instanton methods to the Gross-Pitaevskii equation. Second, we use the truncated Wigner method to study vacuum decay.

First-order phase transitions form an important class of physical phenomena. Typically, these are characterised by metastable, supercooled states and the nucleation of bubbles. Applications range from the condensation of water vapour to the vacuum decay of fundamental quantum fields. In cosmology, bubbles of a new matter phase would produce huge density variations, and unsurprisingly first order phase transitions have been proposed as sources of gravitational waves [1, 2] and as sources of primordial black holes [3, 4].

Clearly a key factor in the relevance of such by-products of phase transitions is the likelihood of that transition occurring. Bubble nucleation rates are exponentially suppressed, and formal estimates of the lifetimes of metastable states can be huge. However, many phase transition rates in ordinary matter are greatly enhanced by the presence of nucleation seeds, in the form of impurities or defects on the boundary of the material. We have argued recently that cosmological bubble nucleation can also be greatly accelerated by nucleation seeds, for example with seeds in the form of primordial black holes [5, 6]. In this paper we propose that seeded bubble nucleation can be studied in a laboratory cold-atom analogue of cosmological vacuum decay [7, 8].

The idea of using analogue systems for cosmological processes comes under the general area of modelling the “universe in the laboratory” [9, 10]. So far, analogue systems have mostly been employed to test ideas in perturbative quantum field theory [11, 12], but nonperturbative phenomena such as bubble nucleation also play an important role in quantum mechanics and field theory.

As pointed out in the classic work of Coleman and others [13–15], the bubble nucleation process in quantum field theory can be described by an *instanton*, or *bounce*, solution to the field equations in imaginary time. The probability for decay is then given, to leading order, by a negative exponential of the action of the instanton. Understanding vacuum decay and the role of the instanton is now particularly pressing in light of the measurements of the Higgs mass, that currently indicates our vacuum is in a region of metastability [16].

The semi-classical description of vacuum decay with gravity involves analytically continuing to imaginary time, and

finding the gravitational instanton. However, while most are comfortable with the assumptions used in perturbative quantum field theory on curved spacetime, such non-perturbative processes are sometimes viewed with more caution. The ability to test such a process via an analogue “table-top” quantum system would be a strong vindication of the use of such techniques. To this end, there have been some recent developments in exploring possible analogue systems that could test vacuum decay. Fialko et al [7, 8] proposed an experiment in a laboratory cold atom system. Their system consists of a Bose gas with two different spin states of the same atom species in an optical trap. The two states are coupled by a microwave field. By modulating the amplitude of the microwave field, a new quartic interaction between the two states is induced in the time-averaged theory which creates a non-trivial ground state structure as illustrated in figure 1 [17].

In this paper we propose an analogue system that can explore the process of catalysis of vacuum decay that is central to our previous results. We use the above model to test seeded vacuum decay by introducing a vortex into the two dimensional spinor Bose gas system. We have used two complementary theoretical approaches. Firstly, we have applied Coleman’s non-perturbative theory of vacuum decay to the Gross-Pitaevskii equation (GPE). Secondly, we have used the truncated Wigner method, a stochastic approach, to study the vacuum decay. In both cases, we find that the introduction of the vortex seed enhances the probability of vacuum decay.

Our system is a two-component BEC of atoms with mass m coupled by a modulated microwave field. The Hamiltonian operator in n dimensions is given by

$$\hat{H} = \int d^n x \left\{ \psi_i^\dagger \left[\frac{-\hbar^2 \nabla^2}{2m} \right] \psi_i + V(\psi_i, \psi_i^\dagger) \right\}, \quad (1)$$

with field operators ψ_i , $i = 1, 2$ and summation over the spin indices implied. Fialko et al. [7, 8] described a procedure whereby averaging over timescales longer than the modulation timescale leads to an interaction potential of the form

$$V = \frac{g}{2} (\psi_i^\dagger)^2 (\psi_i)^2 - \mu \psi_i^\dagger \psi_i - \nu \psi_i^\dagger \sigma_{xij} \psi_j + \frac{g\nu\lambda^2}{4\mu} (\psi_i^\dagger \sigma_{yij} \psi_j)^2, \quad (2)$$

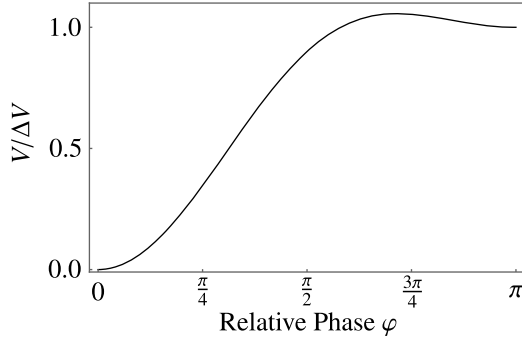


FIG. 1. The field potential V plotted as a function of the relative phase of the two atomic wave functions, φ . The false vacuum is the minimum at $\varphi = \pi$ and the true vacuum the global minimum at $\varphi = 0$. ΔV is the difference in vacuum energy.

where the σ_i are the Pauli matrices. The potential includes the chemical potential μ , point-like interactions of strength g between the field operators and the microwave induced interaction ν . The final term comes from the averaging procedure and introduces a new parameter λ , dependent on the amplitude of the modulation. The trapping potential used to confine the condensate has been omitted in order to isolate the physics of vacuum decay.

The terms proportional to ν are responsible for the difference in energy between the global and local minima of the energy. The global minimum represents the true vacuum state and the local minimum represents the false vacuum. In order to parameterise the difference in energy between the vacua, we introduce a ‘small’ dimensionless parameter ϵ by

$$\epsilon = \left(\frac{\nu}{\mu}\right)^{1/2}. \quad (3)$$

For $\nu > 0$, the true vacuum is a state with $\psi_1 = \psi_2$ and the false vacuum is a state with $\psi_1 = -\psi_2$. The condensate densities of the two components at the extrema are equal to one another, and given by $\langle \psi_1^\dagger \psi_1 \rangle = \langle \psi_2^\dagger \psi_2 \rangle = \rho_m(1 \pm \epsilon^2)$. Note that we prefer to work with the mean density $\rho_m = \mu/g$ rather than the chemical potential. The difference in energy density between the two vacuum states is given by $\Delta V = 4g\rho_m^2\epsilon^2$.

The non-perturbative theory of vacuum decay starts with the imaginary-time partition function

$$Z = \int D\psi_i D\bar{\psi}_i e^{-S[\psi_i, \bar{\psi}_i]/\hbar}, \quad (4)$$

where the integral extends over complex fields ψ_i and their complex conjugates $\bar{\psi}_i$ with action

$$S[\psi_i, \bar{\psi}_i] = \int d^n x d\tau \left\{ \hbar \bar{\psi}_i \partial_\tau \psi_i - \bar{\psi}_i \frac{\hbar^2}{2m} \nabla^2 \psi_i + V(\psi_i, \bar{\psi}_i) \right\} \quad (5)$$

Vacuum decay is associated with instanton solutions to field

equations in imaginary time $\tau = it$ [13, 14]

$$\begin{aligned} \frac{\hbar^2}{2m} \nabla^2 \psi_i - \hbar \partial_\tau \psi_i - \frac{\partial V}{\partial \psi_i} &= 0, \\ \frac{\hbar^2}{2m} \nabla^2 \bar{\psi}_i + \hbar \partial_\tau \bar{\psi}_i - \frac{\partial V}{\partial \bar{\psi}_i} &= 0, \end{aligned} \quad (6)$$

and fields that approach the false vacuum as $r, \tau \rightarrow \infty$.

On the original path integration contour, ψ_i and $\bar{\psi}_i$ are complex conjugates and the field equations imply that the saddle points are static. In order to find the non-static bubble solutions, we have to deform the path of integration into a wider region of complex function space where $\bar{\psi}_i$ is not the complex conjugate of ψ_i . Although this may appear a strange procedure at first sight, this analytic continuation is already implicit in the previous work on vacuum decay as we shall see later.

The full expression for the nucleation rate of vacuum bubbles in a volume \mathcal{V} is [13, 14],

$$\Gamma \approx \mathcal{V} \left| \frac{\det' S''[\psi_b]}{\det S''[\psi_{fv}]} \right|^{-1/2} \left(\frac{S[\psi_b]}{2\pi\hbar} \right)^{N/2} e^{-S[\psi_b]/\hbar}. \quad (7)$$

where S'' denotes the second functional derivative of the action S , and \det' denotes omission of $N = n + 1$ zero modes from the functional determinant of the operator. (For convenience, we always include a constant shift to the action so that the action of the false vacuum is zero.) For seeded nucleation, the volume factor is replaced by the number of nucleation seeds and the number of zero modes becomes $N = 1$. The key feature here is the exponential suppression of the decay rate, and the non-perturbative treatment fails if the exponent is small.

In vacuum decay, the key quantity determining physical aspects of decay is the energy splitting between true and false vacua, ΔV , which is proportional to ϵ^2 . In our system, ϵ also determines the magnitude of the interaction between the two scalars, and for small ϵ , most of the degrees of freedom of the system decouple, leaving an effective field theory of the relative phases of the two condensates as explored in [7, 8] in one spatial dimension.

Here we are interested in seeded decay, so we consider the model in *two* spatial dimensions with polar coordinates r and θ . The natural size of the bubble will be determined by $R_0 = \hbar(\rho_m/m\Delta V)^{1/2}$, and the natural timescale by R_0/c_s , where the sound speed $c_s = (g\rho_m/m)^{1/2}$. To simplify the following analysis, we rescale our dimensionful coordinates accordingly, and also rescale the action:

$$S = \hbar\rho_m R_0^2 \hat{S} \quad (8)$$

Since we are interested in exploring seeded decay, we look for a cylindrically symmetric solution that explicitly highlights the relevant degrees of freedom and includes the possibility of a topologically nontrivial vortex false vacuum state:

$$\begin{aligned} \psi_i &= \rho^{1/2} \left(1 \pm \frac{\epsilon}{2} \sigma \right) e^{\pm i\varphi/2 + in\theta}, \\ \bar{\psi}_i &= \rho^{1/2} \left(1 \pm \frac{\epsilon}{2} \sigma \right) e^{\mp i\varphi/2 - in\theta}, \end{aligned} \quad (9)$$

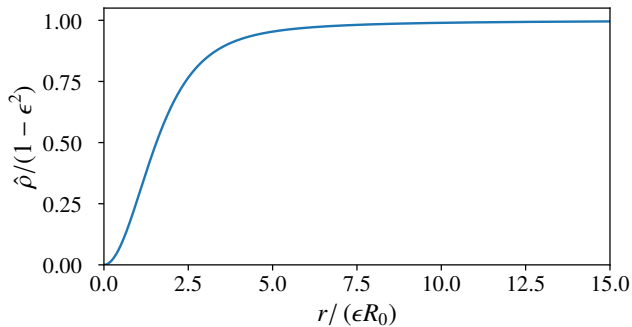


FIG. 2. Vortex density profile $\hat{\rho} = \rho/\rho_m$ plotted as a function of radius r . The density vanishes at the centre and approaches the false vacuum density as $r \rightarrow \infty$. Its physical thickness scales as ϵR_0 .

namely, the relative phase φ between the two components, the leading order (in ϵ) profile of the false vacuum background ρ , an overall common phase winding $n\theta$ that is present in a nontrivial vortex background, and the bubble profile function σ . The upper/lower signs apply to the $i = 1, 2$ spin states respectively.

The pure false vacuum has $n = 0$, and $\rho = \rho_m(1 - \epsilon^2)$, with instanton profiles for φ explored in [7, 8]. Here we are interested in seeded tunnelling, so we also consider the vortex background for $n = 1$, with ρ satisfying the $O(\epsilon^2)$ background equations obtained by substituting (9) in (6). The profile of ρ is precisely that of a superfluid (or global) vortex, and is illustrated in figure 2.

The potential for the instanton solutions depends only on the relative phase φ and the background density ρ . Our rescaling of the length and time coordinates means that we also rescale the potential to $\hat{V} = (V - V_{TV})/2\Delta V$,

$$\hat{V} = \hat{\rho}(1 - \cos \varphi) + \frac{1}{2}\lambda^2 \hat{\rho}^2 \sin^2 \varphi, \quad (10)$$

as plotted in Fig. 1. At zeroth order in ϵ , the field equations (6) imply that $\sigma = -i\hat{\rho}^{-1}\partial_r\varphi$. Note that σ is imaginary, and the bubble solution has $\bar{\psi}_1 \neq \psi_1^\dagger$ as was mentioned earlier. Replacing σ in the action using this field equation gives an action depending only on φ which was used in Refs. [7, 8]. However, at the core of the vortex, $\hat{\rho} \rightarrow 0$ and this replacement of σ is no longer valid. Instead, numerical solutions have been obtained by solving the full equations for the phase φ and the density variation σ .

The vacuum decay rate around a single vortex, using Coleman's formula (7) is

$$\Gamma = A \frac{c_s}{R_0} \left(\frac{\rho_m R_0^2 \hat{S}}{2\pi} \right)^{1/2} e^{-\rho_m R_0^2 \hat{S}}, \quad (11)$$

where A is a dimensionless numerical factor depending on the ratio of determinants (which we do not evaluate here).

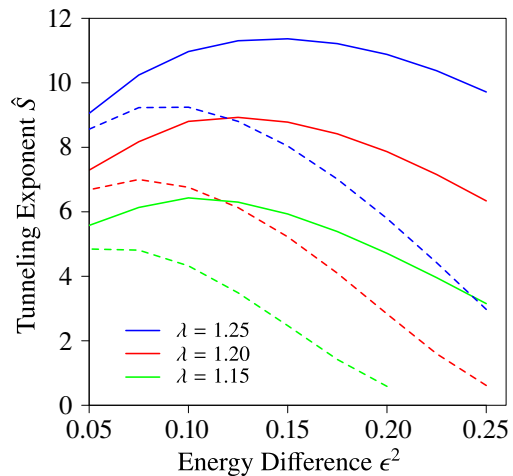


FIG. 3. The dimensionless exponent \hat{S} of the vacuum decay rate plotted as a function of the parameter ϵ^2 . The solid lines represent unseeded vacuum decay and the dashed lines are for bubbles seeded by vortices. The action is lower for the seeded bubbles.

Numerical results for the factor \hat{S} in the decay exponent are shown in Fig 3 [18]. These show clearly that the tunnelling exponent can be reduced significantly in the presence of a vortex. The vortex width from Fig. 2 is related to ϵR_0 . Consequently, smaller values of ϵ are associated with relatively thin vortices compared to the bubble scale R_0 , which have less effect on the vacuum decay rate than vortices with larger values of ϵ .

The nucleation rate depends on the physical parameters through the combination $\rho_m R_0^2$. The length scale R_0 itself is related to the atomic scattering length a_s and the thickness of the condensate a_z via the effective coupling strength g , [19],

$$g = \frac{4\pi\hbar^2}{m} \frac{a_s}{\sqrt{2\pi}a_z}. \quad (12)$$

Thus the factor in the decay exponent becomes $\rho_m R_0^2 = a_z/(4\epsilon^2 \sqrt{8\pi}a_s)$.

As an alternative treatment of bubble nucleation we consider a two-dimensional spinor BEC in a flat-bottomed optical potential. At the mean-field level, the system can be described by the Gross-Pitaevskii equation (GPE) derived from the symmetric Hamiltonian in the rescaled coordinates used above,

$$\frac{i}{\epsilon} \partial_t \psi_i = -\nabla^2 \psi_i + V_T \psi_i + \frac{\partial \hat{V}}{\partial \bar{\psi}_i}. \quad (13)$$

where

$$\frac{\partial \hat{V}}{\partial \bar{\psi}_i} = \frac{1}{2\epsilon^2} \left(\frac{\bar{\psi}_i \psi_i}{\rho_m} - 1 \right) \psi_i - \frac{1}{2} (\sigma_x \psi)_i + \frac{\lambda^2}{4} \frac{\bar{\psi}_i \sigma_y \psi}{\rho_m} (\sigma_y \psi)_i. \quad (14)$$

The truncated Wigner approach seeks to emulate the many-body quantum field description of a BEC with a stochastic description [20, 21]. We compute the false vacuum solution to the GPE, ψ_{iFV} , on a square grid of side L with

M points, creating an initial ensemble of fields by adding noise into unoccupied plane-wave modes according to the zero-temperature prescription $\psi_i = \psi_{iFV} + f(r) \sum_{\mathbf{k}} \beta_{i,\mathbf{k}} e^{i\mathbf{k}\cdot\mathbf{r}}$ for all $|\mathbf{k}| < \pi M/(2L)$, where $\beta_{i,\mathbf{k}}$ are complex gaussian random variables with $\langle \beta_{i,\mathbf{k}}^* \beta_{j,\mathbf{k}'} \rangle = \delta_{i,j} \delta_{\mathbf{k},\mathbf{k}'}/2$. The function $f(r) = \Theta(R-r)/\sqrt{\pi}R$ restricts the noise to the trap interior. We compute the trajectory of each field using the GPE (using a projector to precisely evolve the noise-seeded modes [21]), both with and without initial imprinting of the density and phase profiles of a vortex at the trap centre. The average 1/2 particle per mode of noise in each trajectory emulates vacuum fluctuations.

Numerical results, obtained partly using XMDS2 software [22], confirm that the vortex acts as a nucleation seed when the size of the vortex is of a similar magnitude to the bubble scale R_0 and the particle density ρR_0^2 is not too high, just as we would expect from the non-perturbative results in Fig. 3. In Fig. 4, we demonstrate bubble nucleation around a vortex seed (parameters in figure caption). In an ensemble of 20 stochastic trajectories with an initially imprinted vortex evolved to time $1500R_0/c_s$, the vortex seeds a bubble in 100% of trajectories, but a bubble nucleates spontaneously in the bulk in only 1 trajectory ($\sim 5\%$). In an ensemble of 10 stochastic trajectories with no imprinted vortex evolved to time $2500R_0/c_s$, no spontaneous nucleation within the bulk was observed. This demonstrates the strong enhancement of bubble nucleation by the vortex. We also observe that the walls of the trap strongly enhance bubble nucleation too, both with and without the imprinted vortex. Indeed, we might regard the region outside of the trap, where the phase oscillates widely, as being full of ‘ghost’ vortices. The nucleation process can be triggered by the migration of these ghost vortices into the region just inside the wall. Whilst the wall effect may not be relevant to cosmology, it does introduce a new phenomenon that will be of interest for laboratory BECs. While our simulations represent a proof-of-principle example rather than a concrete experimental proposal, advances in optical trapping [23, 24] and various techniques for vortex imprinting in spinor condensates [25, 26] could be used to probe similar systems experimentally.

In conclusion, our two theoretical approaches, based on the Euclidean field equations (6) and on the truncated Wigner approximation, both show a significant increase of the decay rate of the false vacuum in the presence of a vortex. Numerical simulations also indicate that other kinds of defects, such as the walls of a sharp potential trap, can have a similar effect. Since getting a large enough decay rate is a major difficulty in designing experiments, we expect this to be an important ingredient for putting the theoretical model of [7, 8] into practice, and thus testing vacuum decay in the laboratory.

ACKNOWLEDGEMENTS

We would like to thank Carlo Barenghi for helpful suggestions. This work was supported in part by the Lev-

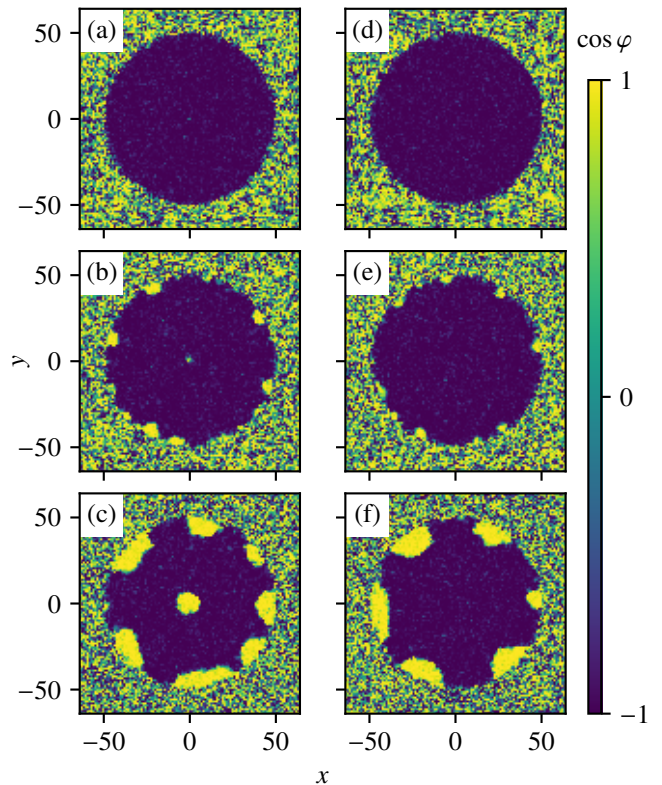


FIG. 4. Typical example of the decay of the false vacuum around a vortex in two dimensions. The plots show the cosine of the relative phase between the two spin states. The BEC is contained inside a circular bucket trap of radius $R = 50R_0$ [$V_T(r) = 5(1 + \tanh(r-R))/(2\epsilon)$], with dimensionless parameters $\lambda = 1.3$, $\epsilon = 0.7$ and $\rho_m R_0^2 = 10.0$. (a) Initially, the false vacuum is contained inside the circular bucket. (b) Later, a bubble of true vacuum (yellow) forms around the vortex in the centre. True vacuum also forms around the walls of the trap. (c) Later still, the true vacuum regions grow, and eventually merge. (d-f) Typical trajectory without an initially imprinted vortex [same times as (a-c)].

erhulme Trust [grant RPG-2016-233], the EPSRC [grant EP/R021074/1], and by the Perimeter Institute. Research at Perimeter Institute is supported by the Government of Canada through the Department of Innovation, Science and Economic Development and by the Province of Ontario through the Ministry of Research and Innovation. RG would also like to thank the Simons Foundation for support and the Aspen Center for Physics for hospitality. FM thanks FAPESP for support and IFSC/USP for its hospitality.

* thomas.billam@ncl.ac.uk
† r.a.w.gregory@durham.ac.uk
‡ florent.c.michel@durham.ac.uk
§ ian.moss@ncl.ac.uk

[1] C. Caprini, R. Durrer, T. Konstandin, and G. Servant, *Phys. Rev. D* **79**, 083519 (2009), arXiv:0901.1661 [astro-ph.CO].

- [2] M. Hindmarsh, S. J. Huber, K. Rummukainen, and D. J. Weir, *Phys. Rev. Lett.* **112**, 041301 (2014), arXiv:1304.2433 [hep-ph].
- [3] S. W. Hawking, I. G. Moss, and J. M. Stewart, *Phys. Rev.* **D26**, 2681 (1982).
- [4] H. Deng and A. Vilenkin, *JCAP* **1712**, 044 (2017), arXiv:1710.02865 [gr-qc].
- [5] R. Gregory, I. Moss, and B. Withers, *JHEP* **03**, 081 (2014), arXiv:1401.0017 [hep-th].
- [6] P. Burda, R. Gregory, and I. Moss, *Phys. Rev. Lett.* **115**, 071303 (2015), arXiv:1501.04937 [hep-th].
- [7] O. Fialko, B. Opanchuk, A. I. Sidorov, P. D. Drummond, and J. Brand, *EPL (Europhysics Letters)* **110**, 56001 (2015), arXiv:1408.1163 [cond-mat.quant-gas].
- [8] O. Fialko, B. Opanchuk, A. I. Sidorov, P. D. Drummond, and J. Brand, *Journal of Physics B Atomic Molecular Physics* **50**, 024003 (2017), arXiv:1607.01460 [cond-mat.quant-gas].
- [9] T. Roger, C. Maitland, K. Wilson, N. Westerberg, D. Vocke, E. M. Wright, and D. Faccio, *Nature Communications* **7** (2016), 10.1038/ncomms13492.
- [10] S. Eckel, A. Kumar, T. Jacobson, I. B. Spielman, and G. K. Campbell, *Phys. Rev.* **X8**, 021021 (2018), arXiv:1710.05800 [cond-mat.quant-gas].
- [11] W. G. Unruh, *Phys. Rev. Lett.* **46**, 1351 (1981).
- [12] C. Barcelo, S. Liberati, and M. Visser, *Living Rev. Rel.* **8**, 12 (2005), [Living Rev. Rel.14,3(2011)], arXiv:gr-qc/0505065 [gr-qc].
- [13] S. R. Coleman, *Phys. Rev.* **D15**, 2929 (1977), [Erratum: *Phys. Rev.* **D16**, 1248(1977)].
- [14] C. G. Callan and S. R. Coleman, *Phys. Rev.* **D16**, 1762 (1977).
- [15] S. R. Coleman and F. De Luccia, *Phys. Rev.* **D21**, 3305 (1980).
- [16] G. Degrassi, S. Di Vita, J. Elias-Miro, J. R. Espinosa, G. F. Giudice, G. Isidori, and A. Strumia, *JHEP* **08**, 098 (2012), arXiv:1205.6497 [hep-ph].
- [17] It has been pointed out that there is an instability in the equations describing the modulated system [27, 28]. However, for the parameters used in this paper and trap radius $25\mu\text{m}$ with ^{39}K , the instability occurs for a modulation frequency $\omega < 800k^2\text{Hz}$, where k is the maximum wavenumber consistent with the equations, in units of the healing length. We will assume that the modulation frequency is above this limit.
- [18] We have checked these results using an ansatz approach akin to that of [29], extended to include dispersion. The results agree within a few per cent.
- [19] M. D. Lee, S. A. Morgan, M. J. Davis, and K. Burnett, *Phys. Rev. A* **65**, 043617 (2002).
- [20] S. Chaturvedi and P. D. Drummond, *European Physical Journal B* **8**, 251 (1999), cond-mat/9801072.
- [21] P. Blakie, A. Bradley, M. Davis, R. Ballagh, and C. Gardiner, *Advances in Physics* **57**, 363 (2008), arXiv:0809.1487 [cond-mat.quant-gas].
- [22] G. R. Dennis, J. J. Hope, and M. T. Johnsson, *Computer Physics Communications* **184**, 201 (2013), arXiv:1204.4255 [physics.comp-ph].
- [23] A. L. Gaunt, T. F. Schmidutz, I. Gotlibovych, R. P. Smith, and Z. Hadzibabic, *Phys. Rev. Lett.* **110**, 200406 (2013), arXiv:1212.4453 [cond-mat.quant-gas].
- [24] G. Gauthier, I. Lenton, N. M. Parry, M. Baker, M. J. Davis, H. Rubinsztein-Dunlop, and T. W. Neely, *Optica* **3**, 1136 (2016), arXiv:1605.04928 [cond-mat.quant-gas].
- [25] Y. Kawaguchi and M. Ueda, *Physics Reports* **520**, 253 (2012), spinor Bose-Einstein condensates, arXiv:1001.2072 [cond-mat.quant-gas].
- [26] D. M. Stamper-Kurn and M. Ueda, *Rev. Mod. Phys.* **85**, 1191 (2013), arXiv:1205.1888 [cond-mat.quant-gas].
- [27] J. Braden, M. C. Johnson, H. V. Peiris, A. Pontzen, and S. Weinfurter, (2018), arXiv:1806.06069 [hep-th].
- [28] J. Braden, M. C. Johnson, H. V. Peiris, and S. Weinfurter, *JHEP* **07**, 014 (2018), arXiv:1712.02356 [hep-th].
- [29] B.-H. Lee, W. Lee, R. MacKenzie, M. B. Paranjape, U. A. Yajnik, and D.-h. Yeom, *Phys. Rev.* **D88**, 085031 (2013), arXiv:1308.3501 [hep-th].